

## Article

# Optimal System Frequency Response Model and UFLS Schemes for a Small Receiving-End Power System after Islanding

Deyou Yang \*, Shiyu Liu and Guowei Cai

School of Electrical Engineering, Northeast Electric Power University, Jilin 132012, China;  
liushiyu2014@163.com (S.L.); caigw@nedu.edu.cn (G.C.)

\* Correspondence: eedyyang@hotmail.com; Tel.: +86-138-4324-7355

Academic Editors: José L. Bernal-Aguatín and Rodolfo Dufo-López

Received: 14 March 2017; Accepted: 26 April 2017; Published: 2 May 2017

**Abstract:** Large frequency deviations after islanding are exceedingly critical in small receiving-end power systems. The under-frequency load shedding (UFLS) scheme is an efficient protection step for preventing system black outs. It is very important to get an exact model to design the UFLS schemes. In this paper, an optimization model to achieve the system frequency response (SFR) model either from the full-scale power system or from test records was proposed. The optimized SFR model took into account the response of governors-prime movers and the dynamic characteristics of loads developed in the modern power system. Then the UFLS schemes were designed via the optimized SFR model and particle swarm optimization (PSO) method. The time-domain simulation with the actual small receiving-end power system was presented to investigate the validity of the presented model and the developed technique.

**Keywords:** System frequency response model; under-frequency load shedding; relay parameters; particle swarm optimization

## 1. Introduction

Because of more economic objectives for operation, power grids are being operated around their stability limits nowadays. Cascading events, such as failures because of the protection system and human errors, can lead to catastrophic blackouts, as revealed by the 14 August 2003 blackout [1]. In general, splitting the system into controlled islands is considered as the last resort against a blackout after large disturbances [2]. A suitable under frequency load shedding (UFLS) scheme is the key to preventing frequency collapse in small receiving-end power systems [3–5].

The concept and model of UFLS schemes for isolated power systems are simple and well known, but it must be robust to prevent frequency collapse against many possible disturbances in the isolated power system. Due to the introduction of electricity markets and to the increasing integration of converter-connected renewable generation [6,7] (e.g., doubly-fed induction generator, DFIG), permanent magnet synchronous generators (PMSG), and photovoltaic (PV)), the power system dynamic frequency responses have recently undergone significant changes. The performance of the UFLS schemes, which are designed based on experience, cannot be necessarily guaranteed in the modern power system. So, several optimization methods have been extensively investigated to design UFLS schemes [3,8–13]. To minimize the amount of shed load, both traditional optimization methods and the evolutionary algorithms have been employed to determine the UFLS relay parameters, i.e., frequency thresholds, step sizes, and time delay. The deterministic optimization algorithms, such as the quasi-Newton method [3], sequential quadratic programming (SQP) [9], and the mixed-integer linear program (MILP) [10] were applied to designing UFLS schemes as effective approaches. Heuristic

methods were also given credit for optimizing UFLS relay parameters. The genetic algorithm (GA) [11] and simulated annealing (SA) [12] were developed for setting UFLS relay parameters successfully.

The design methods for UFLS schemes reported in the literature were almost established on the system frequency response (SFR) model, which was first proposed in [13]. Higher adaptability of the model was advanced by reducing the SFR model to a simplified equivalent SFR model expressed by [14]. Consequently, the performances of the optimized UFLS scheme mainly depends on the precision of the parameters of the SFR model or simplified SFR model except for optimizing strategies. Bogovic et al. used the probability-based approach to analyze the control performance of a traditional UFLS strategy in [15], which is of great significance for promoting the application of traditional UFLS. At the same time, with the rapid development of the modern power system, the complexity of the power system dynamic rose sharply, and the parameters derived by using the conventional static equivalence method were hard to meet the requirements of controlling the scheme design. In recent years, wide area measurement system (WAMS) based adaptive UFLS strategies have been proposed [16]. In particular, Rudez and Mihalic's research [17,18] on WAMS-based UFLS have made important contributions. However, due to the limited numbers of the Phasor Measurement Unit (PMU), the traditional UFLS is still the most widely used in practical engineering at the present stage.

Therefore, this paper describes the development of a parameter identifying strategy based on particle swarm optimization (PSO) [19,20] technology. Then, a model for the design of a robust and high-performance UFLS scheme is proposed based on the simplified SFR model with the identified parameters. In order to achieve the efficiency of the UFLS scheme, the PSO algorithm is also applied to optimize the UFLS relay parameters by capturing the trade-off between minimizing the frequency deviation and the amount of the total load needed to be shed.

PSO is a heuristic algorithm with good properties, and it has been widely applied to solve complex optimization problems in power systems, i.e., stability control, operation, and planning [21,22]. The results based on the time domain simulation with the full-scale power system are presented to demonstrate the precision of the simplified SFR model with the identified parameters and the effectiveness of the proposed optimizing strategies for UFLS scheme design.

Section 2 describes the system model and the proposed formulation used to represent the dynamic frequency response of the power system. The parameter identification strategy for the simplified SFR and UFLS designing models are presented in Section 3. In Section 3.4, the optimized models based on PSO are described. The simulation and results are given in Section 4. Finally, conclusions are offered in Section 5.

## 2. System Model and Formulation

### 2.1. Typical System Frequency Response Model

Figure 1 shows the classical model developed to represent the dynamic frequency response of the power system. The Governor  $i$  represents the model of the speed governor-prime mover of machine  $i$ .  $\Delta\omega$  is frequency deviation,  $\Delta P_L$  is increment of load power,  $\Delta P_G$  is total output of governors, and  $H$  is the equivalent inertia. The Load represents the frequency dependent model of load.

In this general model, the response of the governors-prime movers and the dynamic characteristic of loads are taken into account. The inter machine oscillation is neglected, so the frequency is assumed to be uniform throughout the system. The overall frequency response of the loads is modeled using a single frequency dependent model because of their frequency dependency.

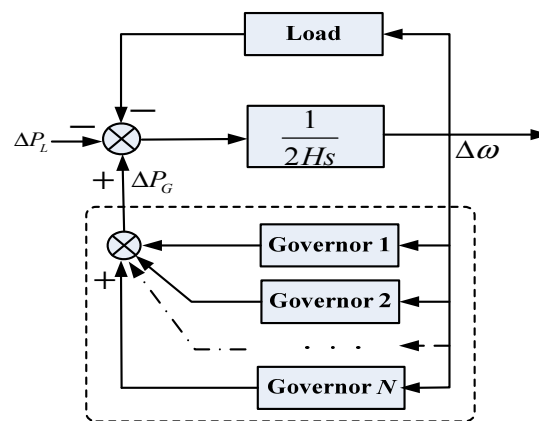


**Figure 1.** Typical model of a power system to analyze the frequency behavior.

## 2.2. Complex Speed Governor-Prime Mover Model

In the published literature, dynamic models have been widely developed and used to adequately depict the behavior of the speed governor-prime movers. Dynamic models of steam turbines are detailed in [23,24] and provide the models of hydraulic turbines. Models of gas turbines are presented in [25]. Other speed governor-prime mover models are also described in [26,27].

Figures 2–4 show the typical models of speed governor-prime movers, respectively: the Institute of Electrical and Electronics Engineers (IEEE) general model for a steam turbine governing system in Figure 2, a typical hydraulic turbine model in Figure 3, and a classical gas turbine model in Figure 4.

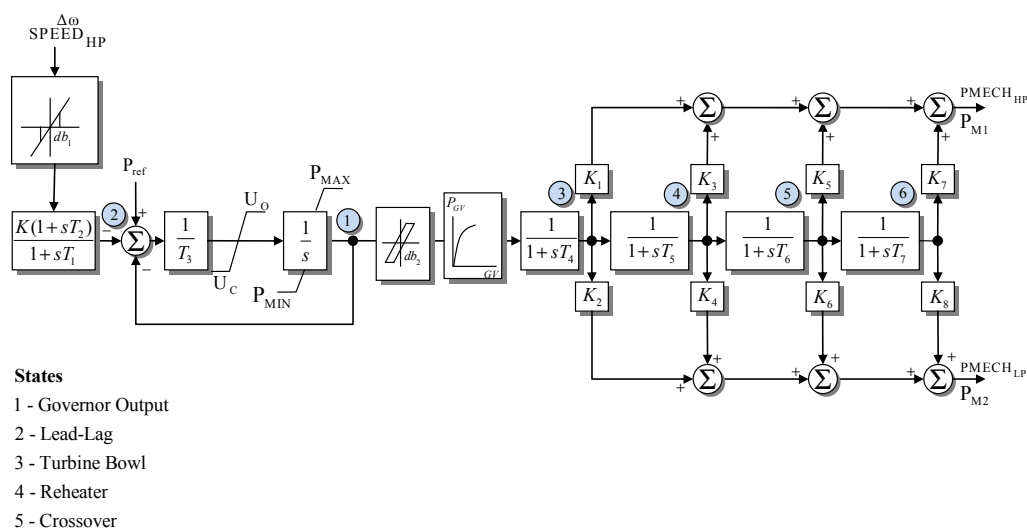


**Figure 2.** General steam turbine speed governing model of IEEE (The parameters are defined in the literature [27]).



Figure 5 shows the composite load model proposed by the Western Electricity Coordinating Council (WECC) [28].

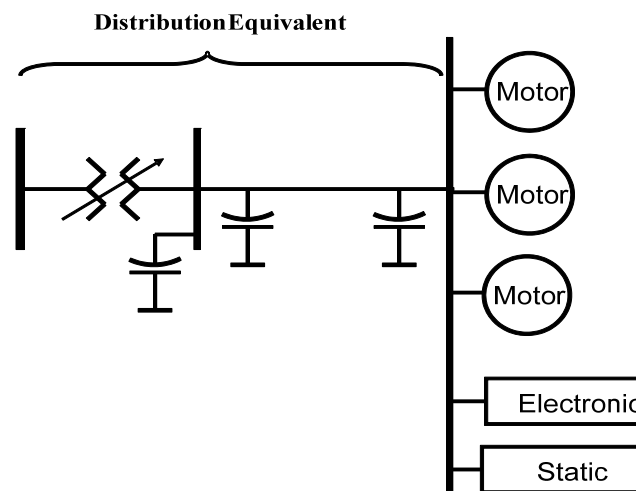


Figure 5. Western Electricity Coordinating Council (WECC) composite load model.

#### 2.4. Simplified System Frequency Response Model Incorporating UFLS

As mentioned before, the dynamic model used to adequately predict the behaviors of a power system are usually very complex, which makes it difficult to obtain a simple analytical model regarding the response of the system frequency and to design the UFLS schemes. In the presented literature, the full scale model is commonly reduced to a simplified equivalent single-machine model in the analysis of the system dynamic frequency behaviors and the UFLS scheme design. This assumption can be accepted for small receiving-end power systems after islanding.

The simplified SFR model incorporating UFLS schemes for a small power system is shown in Figure 6. The simplified SFR model is a single-mass model. The inertias of the different machines are joined in one equivalent inertia. The overall characteristics of the loads due to their frequency dependency is modeled by a single damping factor  $D_L$ , which is the system load frequency damping factor. Governors and prime movers are demonstrated by a short-term first-order model approximation. Generally, the equivalent inertia  $H_e$  and the equivalent gain  $K_e$  of the simplified SFR model can be calculated from the individual generator and governor-prime mover as:

$$H_e = \sum_i \frac{H_i S_i}{S} \quad (1)$$

$$K_e = \sum_i \frac{K_i S_i}{S} \quad (2)$$

where  $H_i$  is the inertia constant of the  $i^{\text{th}}$  generator with a power base  $S_i$  and  $K_i$  is the gain of the  $i^{\text{th}}$  governor-prime mover with a power base  $S_i$ .  $S$  is the system power base.

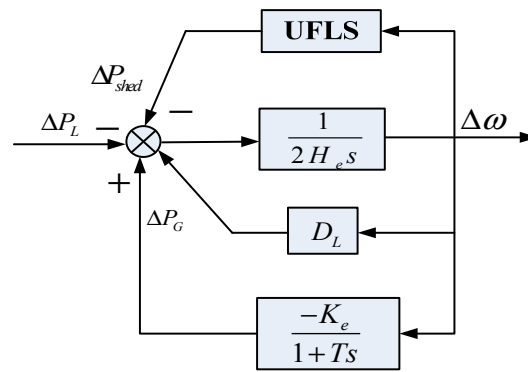


Figure 6. Structure of the simplified SFR model with UFLS.

$T$  is the equivalent time constant of the governor-prime mover and  $\Delta P_{shed}$  is the amount of load shedding. However,  $D_L$  and  $T$  are obtained with difficulty because of the variety of load dynamic behaviors and the different governors-prime movers installed in the different generators. The model and method used to extract the accurate parameters of the simplified SFR model will be proposed in the next section.

### 3. Models for Parameters' Identification and UFLS Schemes' Optimization

#### 3.1. A Review of Particle Swarm Optimization (PSO)

The PSO algorithm was developed by Kennedy and Eberhart in 1995 [19]. PSO is defined as an Evolutionary Computation (EC) method that searches the space to determine the optimal solution for an objective function [20]. The PSO algorithm evaluates itself based on the travels of each particle as well as the swarm cooperation. Each particle starts to traverse randomly accordingly to its own best knowledge and the swarm's experience. The basic regulation of PSO method can be explained by the following:

- (1) Evaluating the objective value of each particle;
- (2) Updating the local and global best objective and positions;
- (3) Updating the velocity and the position of each particle.

For each iteration, the velocity vector of the  $i^{\text{th}}$  particle is updated based on the following Equation:

$$V_i^{(k+1)} = wV_i^{(k)} + c_1r_1(X_{pbest}^{(k)} - X_i^{(k)}) + c_2r_2(X_{gbest}^{(k)} - X_i^{(k)}) \quad (3)$$

In Equation (3),  $w$  is the inertia weight factor,  $V_i^{(k)}$  is the previous velocity of the particle,  $V_i^{(k+1)}$  is the present velocity of the particle,  $c_1$  and  $c_2$  are weighting acceleration constants,  $X_{pbest}^{(k)}$  is the best position that a particle of the group has achieved up to now,  $X_{gbest}^{(k)}$  is the best position that the whole group has achieved up to now, and  $r_1$  and  $r_2$  are random parameters ranging from [0,1], with values produced for each particle in each iteration.

After updating the velocity of the  $i^{\text{th}}$  particle, the particle moves toward its new position from its present position by:

$$X_i^{(k+1)} = X_i^{(k)} + V_i^{(k+1)} \quad (4)$$

Figure 7 illustrates the search processes of the PSO utilizing the modified velocity and position of the individual based on Equations (3) and (4).

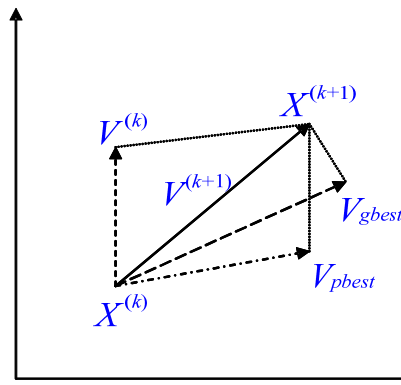


**Figure 7.** The concept of modification of a searching point by Particle Swarm Optimization (PSO).

### 3.2. Parameter Identification Strategy for Simplified SFR

It is well known that accurate parameters are necessary for the design of the protection scheme and parameter identification techniques based on measurements have become mature after many years of development. Accordingly, the parameter identification method for the simplified SFR model is proposed in this section.

For a model with unknown parameters but a known model structure, the parameter identification problem can be regarded as an optimization in which the model output is compared with the actual output. In order to evaluate the parameters to be identified, the actual output is compared with the model output. Generally, the objective function can be defined as a weighted quadratic function:

$$\min g(x) = \frac{1}{m} \sum_{i=1}^m \int_t (y_i - y_i^s)^T W (y_i - y_i^s) \quad (5)$$

$$s.t. \quad lb \leq x \leq ub$$

where  $g(\cdot)$  denotes the objective function,  $W$  is a positive definitive weight matrix,  $y$  is the model output,  $y^s$  is the actual output,  $x$  is the vector of unknown parameters to be identified and  $m$  is the number of recorded data sets.

In the proposed method, the objective function developed as a measure of how the simplified SFR model output satisfies the measurement of the full scale power system output. Then the parameter identification method for the simplified SFR model is formulated as an optimization model:

$$\min g(x) = \frac{1}{m} \sum_{i=1}^m \sum_{k=1}^n (f_i(k) - f_i^s(k))^2, \quad (6)$$

$$s.t. \quad lb \leq x \leq ub$$

The objective function (6) is built with the system frequency response at the center of inertia (COI) [29], and  $x = [H \ D \ K \ T]^T$  are the four unknown parameters to be identified,  $f_i$  and  $f_i^s$  are the system frequency response at the COI of the full scale system output and that of the simplified SFR model output, respectively, and  $n$  is the number of sampled data.

So far, the parameter identification problem for the simplified SFR model has been transformed into an optimization model.

### 3.3. Optimal UFLS Scheme Design

Since the UFLS schemes are desired to be robust and efficient, a quantitative set of design criteria and quantitative performance criteria are considered, shown in the following [9]:

- i. Number of load shedding stages,  $k_{min} \leq k \leq k_{max}$ ;
- ii. Limits on frequency thresholds,  $f_{th\_min}^i \leq f_{th}^i \leq f_{th\_max}^i$ ;

- iii. Range of load shedding sizes for each stage,  $\Delta d_{min} \leq \Delta d^j \leq \Delta d_{max}$ ;
- iv. Range of time delay for each stage,  $t_{d\_min} \leq t_d^j \leq t_{d\_max}$ ;
- v. Margin between two consecutive UFLS threshold frequencies,  $f_{th}^j - f_{th}^{j+1} \geq f_\epsilon$ ;
- vi. Minimum steady state frequency,  $f_{ss} \geq f_{ss\_min}$ ;
- vii. Minimum transient frequency,  $f_{ts}^{min} \geq f_{ts\_min}$ ;
- viii. Maximum transient frequency,  $f_{ts}^{min} \leq f_{ts\_max}$ ;

Thus, the design of the UFLS can be configured into a framework optimization in which the objective function captures the trade-off between the frequency deviations and the amount of the total load shed. Then the optimization model for the robust UFLS scheme design can be described as follows:

$$\min F(Z) = C_e \cdot \int_t \frac{1}{2} \Delta f(t)^2 dt + C_{ls} \cdot \sum_{j=1}^k \Delta d^j, \quad (7)$$

$$\begin{bmatrix} f_{th\_min} \\ \Delta d_{min} \\ t_{d\_min} \end{bmatrix} \leq Z \leq \begin{bmatrix} f_{th\_max} \\ \Delta d_{max} \\ t_{d\_max} \end{bmatrix}, \quad (8)$$

$$\begin{bmatrix} -1 & 1 & \dots & 0 & 0 & 0 & \dots & 0 & 0 & \dots & 0 \\ 0 & -1 & 1 & \dots & 0 & 0 & \dots & 0 & 0 & \dots & 0 \\ \dots & \dots & \dots & \dots & \dots & \dots & \dots & \dots & \dots & \dots & \dots \\ 0 & 0 & \dots & -1 & 1 & 0 & \dots & 0 & 0 & \dots & 0 \\ 0 & 0 & \dots & 0 & 0 & -1 & \dots & -1 & 0 & \dots & 0 \end{bmatrix} \cdot Z \leq \begin{bmatrix} -f_\epsilon \\ \dots \\ \dots \\ -f_\epsilon \\ \Delta d_{max}^s \end{bmatrix} \quad (9)$$

$$\begin{bmatrix} f_{ss\_min} - f_{ss} \\ f_{ts\_min} - f_{ts}^{min} \\ f_{ts}^{max} - f_{ts\_max} \end{bmatrix} \leq 0, \quad (10)$$

The trade-off between minimizing the frequency deviation and the amount of the total load needed to be shed is captured in the developed objective function, shown as Equation (4).  $C_e$  and  $C_{ls}$  are the constant cost coefficient of system energy and load shed, respectively.

As stated in the above description, the design of UFLS schemes can be defined as a standard nonlinear constrained optimization model. The PSO algorithm is applied to solve the optimization problem using Equations (4)–(7).

### 3.4. Solving the Proposed Optimization Model Using PSO

From the above description, it can be seen that parameter identification for the simplified SFR model and the robust UFLS scheme design is a standard nonlinear constrained optimization problem. So, a PSO population-based stochastic search algorithm is used to identify the parameters of the simplified SFR model and design the robust UFLS scheme for the small receiving-end power system after islanding in this paper. The tuning process of a UFLS scheme for a small power system utilizing the PSO algorithm is shown in Figure 8.



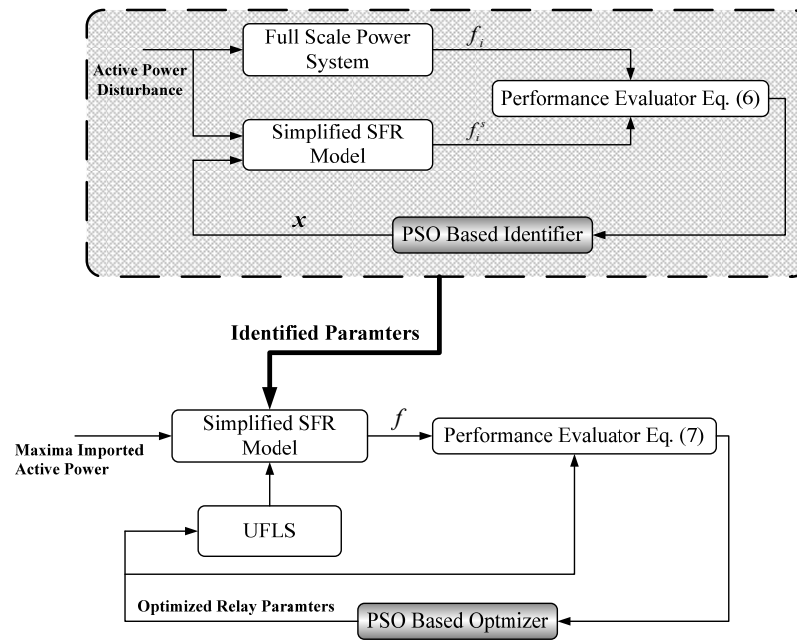


Figure 8. Block diagram of the proposed PSO-based UFLS scheme design.

The following describes the incorporation of the PSO approach for solving the proposed optimization models described in Equations (6) and (7).

- Step 1:** Input PSO parameters, system data, active power disturbance set, the maxima imported active power, and the upper and lower boundaries of each variable.
- Step 2:** Time-domain simulation for a period of 50 s is carried out on the full scale model system to determine the system frequency response at COI for the given contingency set.
- Step 3:** Initialize the swarm comprising the four design parameters,  $x = [H \ D \ K \ T]^T$ , of the simplified SFR model, and relay the parameter  $Z$  of the UFLS scheme, with all parameters satisfying their constraints.
- Step 4:** For each particle in the swarm, the simplified SFR model is used to determine the system frequency response for the given contingency set.
- Step 5:** Evaluate the objective  $g(x)$  of each particle utilizing the objective function in Equation (6).
- Step 6:** Find the best position of each particle,  $p_{best}$ , by comparing the evaluation value of each particle with the one in  $p_{best}$  of the last swarm. If the evaluation value is better, then set  $p_{best}$  as  $g_{best}$ .
- Step 7:** Check the termination condition. If the termination condition is satisfied, go to Step 10.
- Step 8:** The evolved existing population or swarm velocity and position are developed employing Equations (3) and (4).
- Step 9:** Return to Step 4 to repeat the evaluation process with the evolved position.
- Step 10:** Set the latest  $g_{best}$  as the parameters of the simplified SFR model with UFLS.
- Step 11:** Compute the system frequency response using the simplified SFR model with UFLS for each particle in the swarm.
- Step 12:** Evaluate the objective  $F(Z)$  of each particle using the objective function in Equation (7).
- Step 13:** Select the  $g_{best}$  of the relay parameters of the UFLS utilizing the process in Step 6.
- Step 14:** If the termination condition is satisfied, go to Step 17.
- Step 15:** Update the evolved existing swarm velocity and position using Equations (3) and (4).
- Step 16:** Return to Step 11 to repeat the evaluation process with the evolved position.
- Step 17:** The particle that gives the latest  $g_{best}$  has the relay parameters of the optimal UFLS scheme.

#### 4. Simulations and Results

In order to illustrate the developed optimization framework for identifying parameters of the simplified SFR model and designing UFLS schemes, simulations were carried out on the Da Dan power grid. As shown in Figure 9, the Da Dan power grid is a typical small receiving-end power system. The goal is to maximize active power import into the Da Dan power system from the main power network, because the small receiving-end power system has limited local generation but heavy load. Some large disturbances, for instance, a double circuit fault outage on the tie-line between the receiving-end system and the main network, would island the small receiving-end system from the main power system. Robust UFLS schemes must be deployed to safeguard the small receiving-end power system against such large impacts.

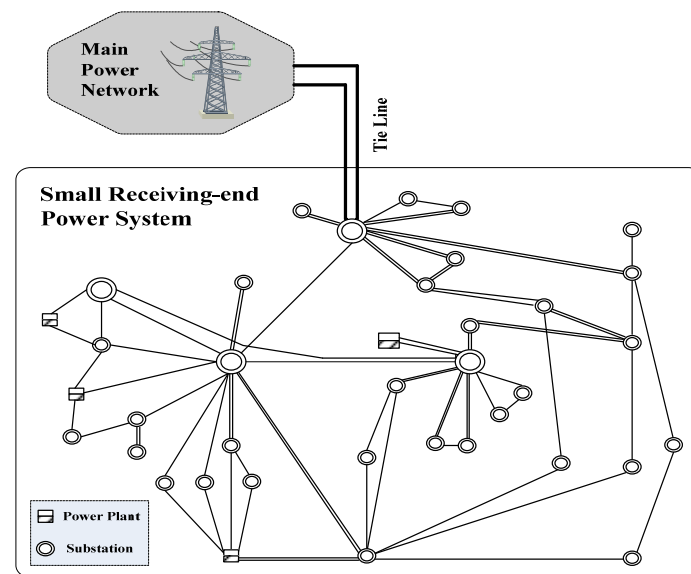


**Figure 9.** Schematic of the Da Dan power grid.

The Da Dan power grid consists of five power plants adding up to 3030 MVA. The imported active power is 800 MW and 1000 MW under valley demand and peak scenarios, respectively, as shown in the following.

The developed technology could be used for practical problems including the identification of parameters for the simplified SFR and the optimal design of UFLS schemes.

The whole optimization procedure was implemented in Matlab 7.1 (The MathWorks, Inc., Natick, MA, USA) and has been executed on an Intel (R) Core (TM) i3 3.2-GHz computer. During the optimization process using PSO, each swarm generation contained 60 position particles. The coefficients in Equation (8),  $\omega$ ,  $c_1$ , and  $c_2$  are set to 0.8, 2, and 2, respectively.

##### 4.1. Identification Parameters of Simplified SFR after Islanding for Small Receiving-End System

The general structure of the simplified SFR model is depicted in Figure 1. This model is widely applied in UFLS scheme designs for small power systems.

Nominal parameters of the generator and governor model in the practical small receiving-end power system are listed in Table 1. In the full scale system simulation, the composite load model (Power System Simulator/Engineering (PSS/E) model) is employed to represent the dynamic characteristics of loads.

**Table 1.** Generator data.

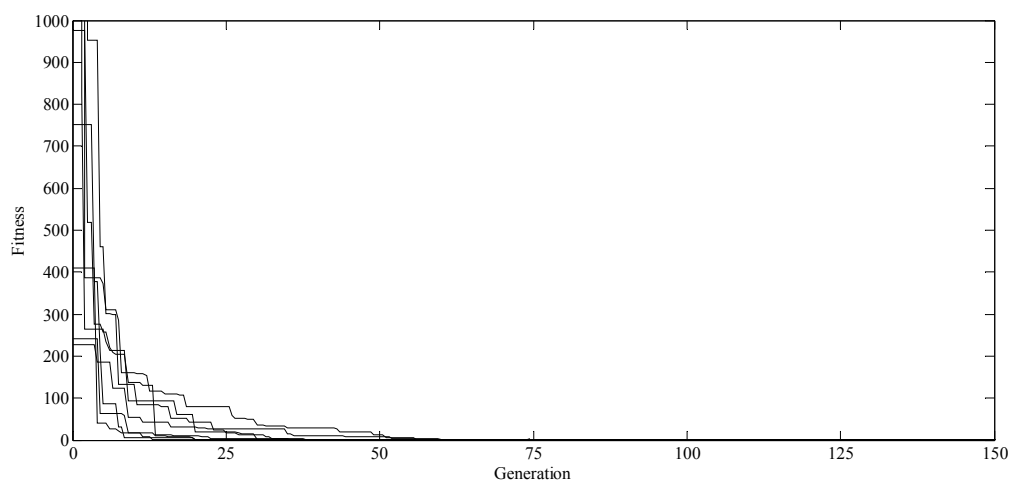
Power Plant	MVA	Inertia Constant	Governor Model in PSS/E
A	$2 \times 150$	14.1	HYGOV
B	$1 \times 330$	4.59	GAST2A
C	$2 \times 600$	2.98	IEEEG1
D	$2 \times 600$	2.39	TGOV5

HYGOV: Hydro Turbine-Governor; GAST2A: Gas Turbine Model Type 2; IEEEG1: IEEE Type 1 Speed-Governing Model; TGOV5: IEEE Type 1 Speed-Governing Model Modified to Include Boiler Controls.

Ten independent runs using PSO were simulated to collect the statistics including the standard deviation, mean, and best and worst optimum results, which are shown in Table 2. Figure 10 shows the optimization process of the presented model for two sample data sets derived from the full scale power system simulation after islanding. The simulation results show that the proposed model converges within 100 generations. The efficiency and accuracy of the proposed model make it useful for applications in parameter identification for the simplified SFR model.

**Table 2.** Statistics of the optimization results for parameter identification.

Best	Worst	Mean	Standard Deviation	Average Run Time (s)
0.1046	0.2118	0.1307	0.0334	1.27

**Figure 10.** PSO optimization process.

The identified parameters are listed in Table 3. At the same time, the parameters obtained by using the static equivalent (SE) and least square (LS) method proposed in [14] are also listed in Table 3 (The system power base  $S$  is the sum of all loads).

**Table 3.** Parameters of the simplified SFR model.

Technology	$H_e$	$D_L$	$K_e$	$T$
SE and LS	2.5501	0.0570	21.07	11.34
PSO	2.3872	0.0632	23.08	13.56
GA	2.5011	0.0485	22.01	12.36

For thoroughly testing the advantages of the proposed PSO-based parameter identification model, the experimental results in Figure 11 compare the performance of the identified model and the static equivalent model with that of the full scale power system. Figure 11a shows the comparative results

under 1000 MW imported active power and Figure 11b under the 800 MW imported condition. Because the performance of the model with the identified parameters matches the results of the full scale system quite well, the advantages of the proposed PSO-based model parameters identification technique are demonstrated. Compared with the equivalent model obtained by using the static equivalent and least square methods, the dynamic frequency responses of the small receiving-end power system can be presented accurately and precisely after islanding.

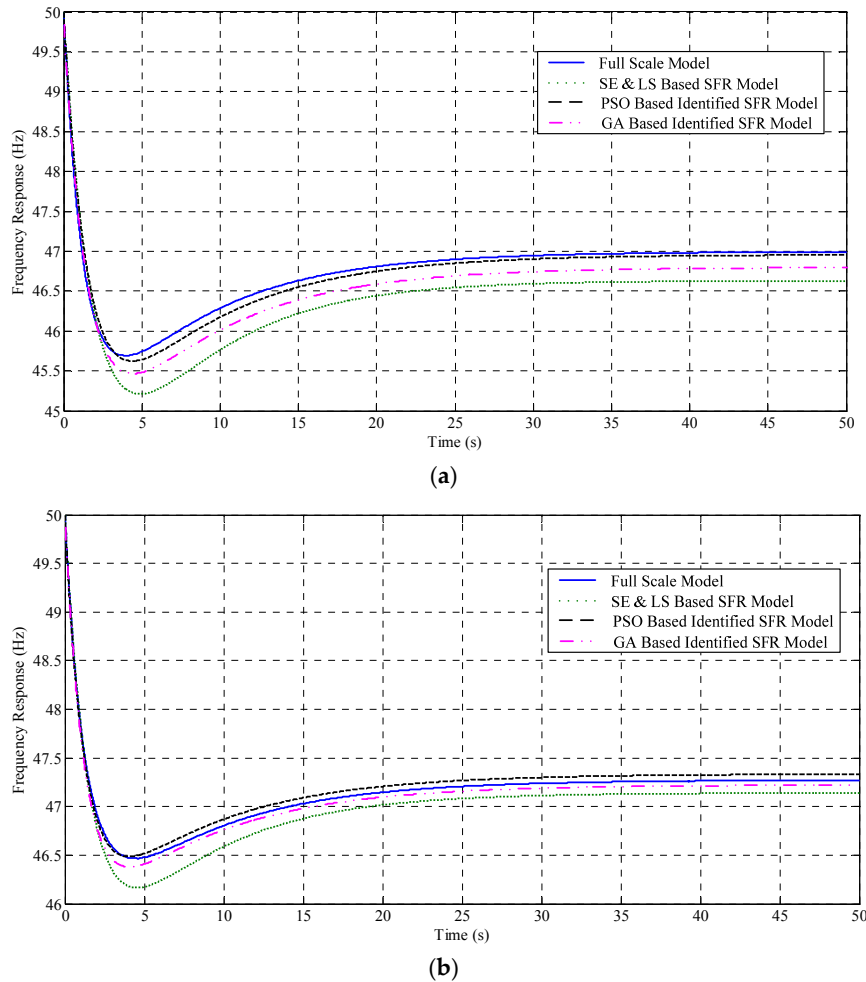


**Figure 11.** Comparison between the full scale model and simplified SFR model response: (a) Peak demand; (b) Valley demand.

#### 4.2. UFLS Design Using the Identified Simplified SFR Model

In this paper, the main concern is to optimize the UFLS schemes to maximize the imported power under normal circumstances and yield acceptable system performance after islanding for the small receiving-end power system. To ensure the UFLS schemes against accidents or the loss of the maximized active power import, the PSO-based model proposed in Section 3 was employed to minimize the frequency deviations and the total amount of the load needed to be shed.

In order to illustrate the proposed approach for designing UFLS schemes, we considered the small receiving-end system shown in Figure 10 whose simplified SFR model parameters are identified using the developed model. Other parameters are set as:  $C_e = 1.0$  pu/pu,  $C_{ls} = 0.1$  pu/pu [9];  $k_{min} = 1$ ,  $k_{max} = 6$ ;  $f_{th\_min} = 48.0$  Hz,  $f_{th\_max} = 49.5$  Hz;  $f_\epsilon = 0.1$  Hz;  $\Delta d_{max} = 0.3$  pu,  $\Delta d_{min} = 0.01$  pu;  $t_{d\_min} = 0.1$  s,  $t_{d\_max} = 0.2$  s;  $f_{ss\_min} = 49.8$  Hz,  $f_{ts\_min} = 48.8$  Hz,  $f_{ts\_max} = 50.2$  Hz.

Table 4 shows the statistical optimization results for different  $k$  by performing ten independent runs. As seen, the most favorable UFLS schemes are for  $k = 3$ . Table 5 shows the optimized relay setting of the UFLS schemes for the test system on the condition that the imported active power is maximized. Only the first two ranked values of the load shedding stages are shown in Table 5.

**Table 4.** Statistics of the optimization results for the UFLS design.

Number of Load Shedding Stages	Best	Worst	Mean	Standard Deviation	Average Run Time (s)
2	1.864	2.061	1.962	0.047	2.27
3	1.285	1.468	1.307	0.032	6.63
4	1.517	1.736	1.594	0.054	10.78
5	1.717	2.014	1.885	0.068	15.32
6	2.134	2.387	2.205	0.073	20.25

**Table 5.** Optimized UFLS schemes.

Stage	Number of Load Shedding Stages					
	3			4		
	$f_{th}$	$\Delta d$	$t_d$	$f_{th}$	$\Delta d$	$t_d$
	(Hz)		(s)	(Hz)		(s)
1	49.50	7.52%	0.1	49.5	6.62%	0.13
2	49.31	9.70%	0.1	49.3	7.11%	0.15
3	49.11	6.25%	0.1	49.1	3.88%	0.10
4	—	—	—	48.9	5.89%	0.14
5	—	—	—	—	—	—
6	—	—	—	—	—	—
Obj	1.285			1.517		

#### 4.3. Time Domain Verification of the Optimal UFLS Schemes

In this part, the designed optimal UFLS schemes in the afore-mentioned section were applied to the full scale small receiving-end system. The system dynamic frequency responses of the full scale system for disturbance events are simulated using the DSA Tool software [30].

For this simulation, the performances of Scheme A designed using the SE and LS based SFR model, Scheme B designed using the GA based identified SFR model, and Scheme B designed using the PSO based identified SFR model are compared. The system frequency responses of the full scale system with the designed optimal UFLS schemes for the contingencies computed with the DSA Tool software are shown in Figure 12. The numerical comparisons of different UFLS schemes are also given in Table 6.

**Table 6.** Performance of the different UFLS schemes.

Condition	Peak Demand			Valley Demand		
Scheme	A	B	C	A	B	C
Amount of Load Shed (MW)	781.2	809.7	829.8	642.3	628.6	607.9
Steady Frequency (Hz)	49.88	79.89	49.90	49.96	49.91	49.88
Minimum Frequency (Hz)	48.92	48.85	48.81	49.09	49.10	49.02

By means of the designed optimal UFLS schemes utilizing the proposed PSO-based model, the system frequency response trajectory for two contingencies is shown in Figure 12. It is shown in Figure 12 that the designed optimal UFLS schemes bring the system back to the safe region of [49.8Hz,

50.2Hz] (the shadowed part in Figure 12) after islanding. The results also show that the system frequency does not settle above 50 Hz and does not exceed the safe range.

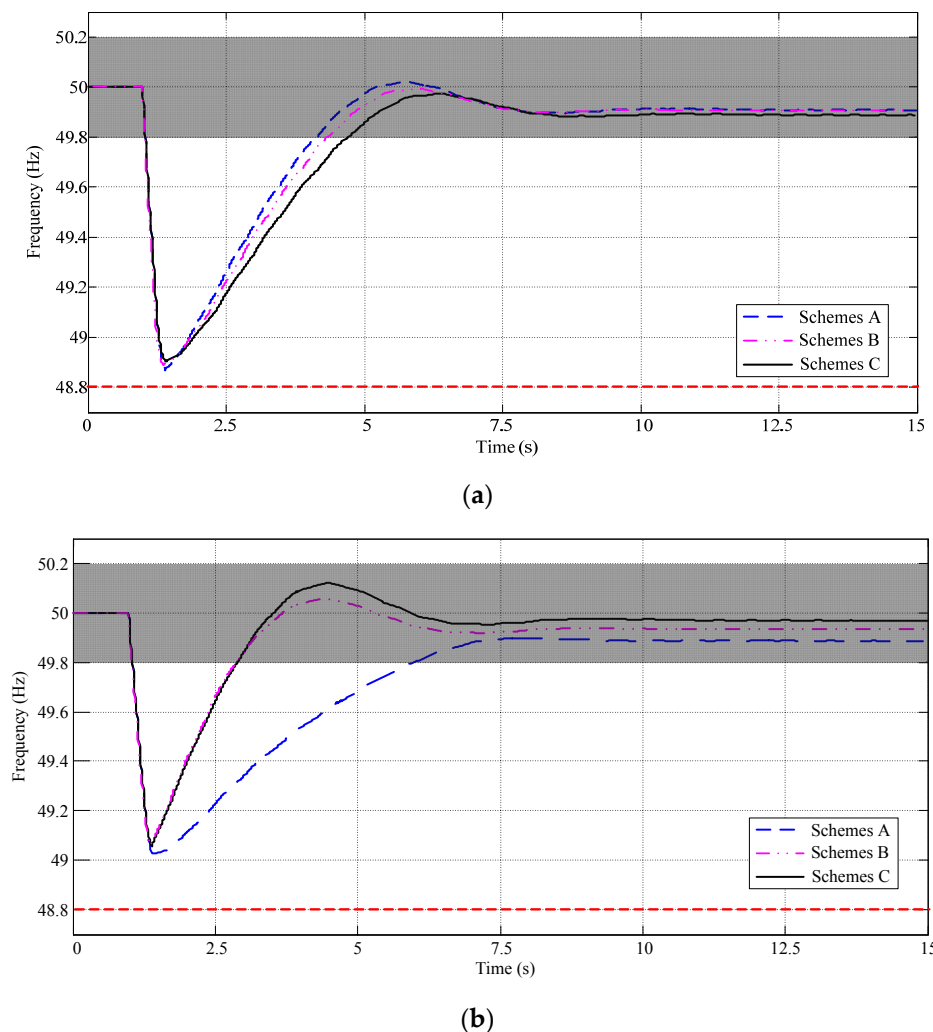


**Figure 12.** System frequency responses with optimized UFLS schemes under different conditions: (a) Peak demand; (b) Valley demand.

As shown in Figure 12, the optimized UFLS schemes derived using the PSO based, identified simplified SFR model for two disturbances in the small receiving-end system performs better than the UFLS schemes designed using the SE and LS based SFR model. On the other hand, as depicted in Table 6, the optimized UFLS schemes obtained using the PSO based, identified simplified SFR model have advantages of the set rules to guard the security system and thus minimize the total load that is needed to be shed for the islanded system. The results also show that the optimal UFLS schemes derived from the PSO based, identified simplified SFR model have better robustness.

In general, the optimized UFLS schemes derived utilizing the PSO based, identified simplified SFR model and the developed PSO-based UFLS schemes optimizing model gave better performances for the same contingency event, as shown in Figure 12a,b.

## 5. Conclusions

In this paper, novel methods based on PSO are presented for parameter identification and UFLS design with a nonlinear optimal model structure. In the first instance, the PSO-based model parameters identification technique was developed to determine the parameters of the simplified SFR model from

the dynamic responses of the full-scale system model. Then, an optimal framework based on PSO for setting the optimal relay parameters of the UFLS schemes using the identified simplified SFR model was developed. Simulations carried out on a practical small receiving-end power system are provided to indicate how the optimal UFLS schemes that are designed protect the small receiving-end system after islanding. It is shown that the proposed optimization setup can be easily applied for practical applications. Finally, the results derived from the time domain simulation of the small scale power system were shown to validate the effectiveness of the proposed PSO-based model.

**Acknowledgments:** This work is supported by the National Nature Science Foundation of China (No. 51507028) and “Thirteen five” Science and Technology Projects of The Education Department of Jilin Province (No. JJKH20170100KJ).

**Author Contributions:** Yang Deyou and Cai Guowei conceived and designed the experiments; Liu Shiyu performed the experiments; Yang Deyou and Liu Shiyu analyzed the data; Yang Deyou and Liu Shiyu wrote the paper.

**Conflicts of Interest:** The authors declare no conflict of interest.

## References

1. U.S. Canada Power System Outage Task Force. Final Report on the 14 August 2003 Blackout in the United States and Canada: Causes and Recommendation. Available online: <https://reports.energy.gov/> (accessed on 2 May 2004).
2. Sun, K.; Hur, K.; Zhang, P. A new unified scheme for controlled power system separation using synchronized phasor measurements. *IEEE Trans. Power Syst.* **2011**, *3*, 1544–1554. [[CrossRef](#)]
3. Halevi, Y.; Kottick, D. Optimization of load shedding system. *IEEE Trans. Energy Convers* **1993**, *6*, 207–213. [[CrossRef](#)]
4. Concordia, C.; Fink, L.H.; Poullikas, G. Load shedding on an isolated system. *IEEE Trans. Power Syst.* **1995**, *3*, 1467–1472. [[CrossRef](#)]
5. Huang, C.-C.; Huang, S.J. A time-based load shedding protection for isolated power systems. *Electr. Power Syst. Res.* **1999**, *11*, 161–169. [[CrossRef](#)]
6. Rouco, L.; Zamora, J.; Egidio, I.; Fernández-Bernal, F. Impact of Wind Power Generators on the Frequency Stability of Synchronous Generators. In Proceedings of the Cigré Session 2008, Paris, France, 24–29 August 2008.
7. Tan, Y. Impact on the Power System with a Large Penetration of Photovoltaic Generation. Ph.D. Thesis, University of Manchester Institute of Science and Technology, Manchester, UK, 2004.
8. Lokay, H.E.; Burtnyk, V. Application of under frequency relays for automatic load shedding. *IEEE Trans. Power App. Syst.* **1968**, *2*, 776–783. [[CrossRef](#)]
9. Hau, A.D.L. A general-order system frequency response model incorporating load shedding: Analytic modeling and applications. *IEEE Trans. Power Syst.* **2006**, *2*, 709–717.
10. Ceja-Gomez, F.; Qadri, S.S. Under-frequency load shedding via integer programming. *IEEE Trans. Power Syst.* **2012**, *3*, 1387–1394. [[CrossRef](#)]
11. Lopes, J.A.P. Optimum determination of under frequency load shedding strategies uses a genetic algorithm approach. In Proceedings of the Annual North American Power Symposium, Waterloo, ON, Canada, 23–24 October 2000.
12. Sigrist, L.; Egidio, I.; Rouco, L. A method for the design of ufls schemes of small isolated power systems. *IEEE Trans. Power Syst.* **2012**, *2*, 951–958. [[CrossRef](#)]
13. Anderson, P.M.; Mirheydar, M. A low-order system frequency response model. *IEEE Trans. Power Syst.* **1996**, *3*, 720–729. [[CrossRef](#)]
14. Egidio, I.; Fernández-Bernal, F.; Centeno, P. Maximum frequency deviation calculation in small isolated power systems. *IEEE Trans. Power Syst.* **2009**, *4*, 1731–1738. [[CrossRef](#)]
15. Bogovic, J.; Rudez, U.; Mihalic, R. Probability-based approach for parametrization of traditional under frequency load-shedding schemes. *IET Gener. Transm. Distrib.* **2015**, *16*, 2625–2632. [[CrossRef](#)]
16. De la Ree, J.; Centeno, V.; Thorp, J.S.; Phadke, A.G. Synchronized phasor measurement applications in power systems. *IEEE Trans. Smart Grid* **2010**, *1*, 20–27. [[CrossRef](#)]

17. Rudez, U.; Mihalic, R. Analysis of under frequency load shedding using a frequency gradient. *IEEE Trans. Power Deliv.* **2011**, *2*, 565–575. [[CrossRef](#)]
18. Rudez, U.; Mihalic, R. WAMS-based underfrequency load shedding with short-term frequency prediction. *IEEE Trans. Power Deliv.* **2016**, *4*, 1912–1920. [[CrossRef](#)]
19. Kennedy, J.; Eberhart, R. Particle swarm optimization. In Proceedings of the IEEE International Conference on Neural Networks, Perth, Australia, 27 November–1 December 1995.
20. Kennedy, J.; Eberhart, R. *Swarm Intelligence*; Morgan Kaufmann Publishers: San Francisco, CA, USA, 2001.
21. Cheng, P.; Peng, B.; Liu, Y.; Cheng, Y.; Huang, J. Optimization of a fuzzy-logic-control-based mppt algorithm using the particle swarm optimization technique. *Energies* **2015**, *6*, 5338–5360. [[CrossRef](#)]
22. Del Valle, Y.; Venayagamoorthy, G.K.; Mohagheghi, S. Particle swarm optimization: basic concepts, variants and applications in power systems. *IEEE Trans. Evolut. Comput.* **2011**, *1*, 171–195. [[CrossRef](#)]
23. DeMello, F.P. Dynamic models for fossil fueled steam units in power system studies. *IEEE Trans. Power Syst.* **1991**, *2*, 753–761.
24. IEEE Working Group on Prime Mover and Energy Supply Models for System Dynamic Performance Studies. Hydraulic turbine and turbine control models for system dynamic studies. *IEEE Trans. Power Syst.* **1992**, *1*, 167–179.
25. Kola, V.; Bose, A.; Anderson, P.M. Power plant models for operator training simulators. *IEEE Trans. Power Syst.* **1989**, *2*, 559–565. [[CrossRef](#)]
26. Pereira, L.; Kosterev, D.; Davies, D.; Patterson, S. New thermal governor model selection and validation in the WECC. *IEEE Trans. Power Syst.* **2004**, *2*, 517–523. [[CrossRef](#)]
27. Dynamic Models for PSS®Software Product Suite. Available online: [http://www.energy.siemens.com/hq/pool/hq/services/power-transmission-distribution/power-technologies-international/software-solutions/BOSL\\_Controller\\_Standard-1.pdf](http://www.energy.siemens.com/hq/pool/hq/services/power-transmission-distribution/power-technologies-international/software-solutions/BOSL_Controller_Standard-1.pdf) (accessed on 29 April 2017).
28. Kosterev, D.; Meklin, A. Load modeling in WECC. In Proceedings of the Power Systems Conference and Exposition, Atlanta, Georgia, 29 October–1 November 2006.
29. Kundur, P. *Power System Stability and Control*; McGraw-Hill, Inc.: New York, NY, USA, 1994.
30. *DSA Manager User Manual*; Powertech Labs Inc.: Surrey, BC, Canada, 2006.



© 2017 by the authors. Licensee MDPI, Basel, Switzerland. This article is an open access article distributed under the terms and conditions of the Creative Commons Attribution (CC BY) license (<http://creativecommons.org/licenses/by/4.0/>).